

$f_2(1270) \rightarrow \pi + \pi$ as a Probe of Spin and Vorticity in Heavy-Ion Collisions

In Woo Park,^{1,*} Beomkyu Kim,^{2,†} Giorgio Torrieri,^{3,‡} Kayman J. Gonçalves,^{3,§} Sanghoon Lim,^{4,¶} and Su Hyoung Lee^{1, **}

¹Department of Physics and Institute of Physics and Applied Physics, Yonsei University, Seoul, Korea

²Department of Physics, Sungkyunkwan University, Suwon, Korea

³Universidade Estadual de Campinas, Instituto de Física Gleb Wataghin Rua Sergio Buarque de Holanda 777, Campinas, São Paulo, Brazil

⁴Department of Physics, Pusan National University, Pusan, Korea

(Dated: February 2, 2026)

The correlation between vorticity and spin alignment in heavy-ion collisions can be probed through polarization measurements of hadrons, whose total spin originates from both constituent-quark spins and orbital angular momentum in the quark-model framework. To motivate such experimental studies, we calculate the general angular distribution of produced pion in $f_2(1270) \rightarrow \pi + \pi$ using interaction Lagrangian and helicity formalism and check that both methods yield the same result. The distribution is given as a function of angle between pion and initial quantization axis of f_2 and the spin density matrix element of f_2 . Its diagonal entries and ρ_{20} component were computed assuming local thermal equilibrium and blast wave model for different centrality classes, hence given as a function of azimuthal angle with respect to the impact parameter.

I. INTRODUCTION

In non-central heavy ion collisions, a huge global orbital angular momentum (OAM) of the order of $10^5 - 10^7 \hbar$ is generated. The generated OAM is partially transferred to the spin polarization of quarks and anti-quarks through spin-orbit coupling, resulting in the global polarization of the hadrons along the OAM. The global spin polarization of Λ hyperon was measured through a self analyzing weak decay $\Lambda \rightarrow p + \pi$ [1]. On the other hand, the measurement of vector meson spin alignment was done through its strong p -wave decay into two pseudoscalar mesons such as $\phi \rightarrow K^+ K^-$, $K^* \rightarrow K\pi$ [2–4] and $D^* \rightarrow D\pi$ [5].

In a thermal environment the polarization is given by the trace over the thermalized density matrix

$$P_h = \text{Tr}(\hat{S}_z \cdot \hat{\rho}) \quad , \quad \hat{\rho} = \frac{1}{Z} \exp \left[\frac{\hat{S} \cdot \hat{\Omega}}{T} \right] \quad , \quad Z = \text{Tr}(\hat{\rho}) \quad (1)$$

where \hat{S} is the spin vector in the right representation (spinor, vector, tensor etc), $\hat{\Omega}$ is the vorticity, and we define the z direction as the one we want to measure (usually experimentalists measure the global polarization perpendicular to the impact parameter, local polarization in the beam direction, jet polarization in the jet plane).

Note that [6] weak decays allow us to measure polarization P_h , but strong decays are parity-conserving, therefore they only allow us to measure spin alignment, $\sim P_h^2$. Nevertheless, if the system is in thermal equilibrium, Eq. (1) should allow the calculation of the spin alignment of all particles just from the two parameters of Ω and T .

However, there are very good reasons to think that equilibrium between spin and vorticity is imperfect [7]. At most, the spin density $s_{\alpha\beta}$ and the vorticity $\Omega_{\alpha\beta}$ combine in a relativistic Fert-Valet type equation governed by a time-scale τ_Ω , related to the vortical susceptibility χ by a fluctuation-dissipation type relation [8–10] given as

$$\tau_\Omega u_\alpha \partial^\alpha s_{\mu\nu} + s_{\mu\nu} = \chi \Omega_{\mu\nu}, \quad (2)$$

in which case there are indications [10, 11] that τ_Ω is of the order of the lifetime of the fireball.

In this case, the formula Eq. (1) cannot be the full story, since spin and angular momentum carried by vorticity somehow combine to produce a hadron density matrix. For a quark model coalescence, conservation of angular momentum imposes a formula [12] dependent on one unknown “decoherence” parameter $P_L(\omega)$, the probability of a vortex with vorticity ω to give the hadron L of angular momentum, and Clebsch-Gordan coefficients and $6-j$ symbols. In the quark coalescence model, conservation of angular momentum leads to an expression [12] that depends on a single unknown decoherence parameter, $P_L(\omega)$. This quantity represents the probability that a vortex with vorticity ω produces a hadron with total angular momentum L . The resulting formula involves appropriate Clebsch-Gordan coefficients and Wigner $6-j$ symbols. For a meson this will be

$$(\hat{\rho}^M)^L_{m', m''} = \sum_{m'', m} \sum_{m'_1, m'_2, m'_L} \sum_{m_1, m_2, m_L} P_L(\omega) d^j_{m' m''}(v) C^{j, m''}_{S_1 + S_2, m'_1 + m'_2, L, m'_L} C^{S_1 + S_2, m'_1 + m'_2}_{S_1, m'_1, S_2, m'_2} C^{j, m}_{S_1 + S_2, m_1 + m_2, L, m_L} C^{S_1 + S_2, m_1 + m_2}_{S_1, m_1, S_2, m_2} \rho^1_{m_1, m'_1}(\Omega) \rho^2_{m_2, m'_2}(\Omega) \left[d^j_{mm''}(v) \right]^{-1}, \quad (3)$$

here v is the coalescence angle, and the quark density matrices are given by Eq. (1). $d^j(v)$ is Wigner d-matrix of spin j . For baryons, the formula is more complicated but of the same type, see [13] for details. The diagonal elements of the

* inwoopark95@gmail.com

† kimbyumkyu@skku.edu

‡ torrieri@unicamp.br

§ kaymanjhosef10@gmail.com

¶ shlim@pusan.ac.kr

** suhoungh@yonsei.ac.kr

density matrix for different centrality classes are calculated assuming thermal production [Eq. (1)] and are presented as functions of the angle with respect to the impact parameter. The calculations are performed within a blast-wave framework incorporating elliptic flow and polarization effects [14, 15], together with a global vorticity as modeled in Ref. [16]. For quantitative comparisons with experimental data, blast-wavetype models such as that of Ref. [13] are required.

As argued in [12] particles of higher spin than 1/2, carrying more than one qubit of information, are optimal probes of such non-equilibrium. This is because the angular distribution of decay products in the hadron rest frame, $W(\theta, \phi, \rho_{ij})$ (where θ is aligned with the spin and ϕ is perpendicular to it) is related to the density matrix elements by a simple partial wave analysis (see the next section for an example), allowing us direct access to *most* (or all, for weak decays) ρ_{ij} matrix elements, including the diagonal ones.

Of course, the decay frame (θ, ϕ, p_T^*) is generally different from the lab frame (θ_r, ϕ_r, p_T) . For non-relativistic particles, the difference in frames is simplified by the approximate invariance of the angles, so the final distribution in lab coordinates is simply a convolution.

$$\frac{dN}{d\Omega} = \int p_T dp_T dy d\phi \left(\frac{dN_{\text{parent}}}{p'_T dp'_T dy' d\phi'} \right) \Big|_{y'=y, p'_T=p_T, \phi'=\phi} \times \frac{\partial(y, p_T, \phi)}{\partial(\theta_r, \phi_r, p)} W(\theta, \phi, \rho_{ij}(\theta_r, \phi_r)), \quad (4)$$

where $W(\theta, \phi, \rho_{ij}(\theta_r, \phi_r))$ will be calculated in the next section using a phenomenological Lagrangian and the helicity formalism. For Bjorken type dynamics where coalescence is local in rapidity, the momentum and ϕ parts of the Jacobian are just normalization parameters so

$$\frac{\partial(\eta, p_T, \phi)}{\partial(\theta_r, \phi_r, p)} \propto \frac{d\theta_r}{d\eta} \quad , \quad \eta \simeq \tanh^{-1} \cos\left(\frac{\theta_r}{2}\right). \quad (5)$$

Concretely, we know that there are two potential sources of vorticity common to all events: a “global” vorticity, which is common to the whole event and is formed at the initial collision due to the finite impact parameter, and “local” vorticity which is formed in concomitance with elliptic flow (Fig. 1). If τ_Ω in Eq. (2) is indeed comparable to the lifetime of the fireball, then one expects spin to be more aligned in the global direction, while vorticity to be a sum of global and local directions (Fig 1). While a numerical calculation is needed for quantitative modeling, it is clear that this will give substantial differences between a density matrix of the form Eq. (1) and one of the form Eq. (3).

In this work, we wish to concentrate on $f_2(1270)$, which is interesting in this regard for several reasons. It is a tensor ($S = 2$) meson, whose density matrix is very large, 5×5 . Even in a parity preserving decay we can obtain more information than spin alignment, since we can distinguish $\rho_{0,0}$ from $\rho_{\pm 1, \pm 1}$ and $\rho_{\pm 1, \pm 1}$ from $\rho_{\pm 2, \pm 2}$ as well as identify the non-diagonal matrix elements using the expressions for the

whole spherical harmonic coefficients.¹ It should be noted that the $\pi - \pi$ invariant mass distribution of $f_2(1270)$ was recently measured by the ALICE collaboration using central-exclusive production events in pp collisions [17]. Although the background conditions in heavy-ion collisions are expected to be significantly different, this measurement provides a valuable baseline and serves as a natural starting point for future studies in heavy-ion collision systems.

Moreover, according to the quark model, it is an $L = 1$ angular momentum state, which, if the picture in [12] is correct, should be particularly affected by vorticity (similarly to quarkonium [18]).

Furthermore, spin alignment *has* to be either aligned ($L = 1$) or anti-aligned ($L = 3$) for this particle to form. Thus, $P_L(\omega)$ here appears only as a normalization parameter (quarks in a misaligned spin and angular momentum state do not coalesce into f_2). Thus, both the abundance and the spin alignment of f_2 mesons, when compared to the abundance and polarization/alignment of other hadrons, is a promising probe of the dynamics between spin and vorticity.

For these reasons, the f_2 meson is a particularly “clean” probe for ascertaining if hadronization of spin is truly thermal (Eq. (1)), of coalescence type (Eq. (3)) or perhaps of another form. In the rest of this paper we will investigate this quantitatively.

This paper is organized as follows. In Section II, we evaluate the coupling strength between the f_2 and π mesons in the $f_2 \rightarrow \pi + \pi$ (*d-wave* decay) using an effective Lagrangian interaction. We then calculate the general angular distribution of the pions produced in the decay $f_2 \rightarrow \pi + \pi$ using both the Lagrangian interaction formalism and the helicity formalism, and verify that the two methods yield identical results. In Section III, we introduce the parametrization of the elliptic fluid flow which accounts for the effects of the elliptic flow in the expanding medium. Furthermore, we use the anisotropic fluid flow parametrization to evaluate the fluid thermal vorticity. In Section IV, we present the plot of the diagonal matrix element and ρ_{20} of the spin density matrix of f_2 without and with global vorticity, as a function of the azimuthal angle in the $x - y$ plane for various classes of events centrality assuming thermal production.

II. THE DECAY WIDTH AND ANGULAR DISTRIBUTION OF $f_2 \rightarrow \pi + \pi$

To describe the decay $f_2(p) \rightarrow \pi(p_1) + \pi(p_2)$, we adopt the interaction Lagrangian introduced in Refs. [19, 20].

$$\mathcal{L}_{f_2\pi\pi} = -\frac{2g_{f_2\pi\pi}}{m_{f_2}} \partial_\mu \pi \cdot \partial_\nu \pi f_2^{\mu\nu}. \quad (6)$$

¹ Perhaps a good name for such a measurement is spin projection

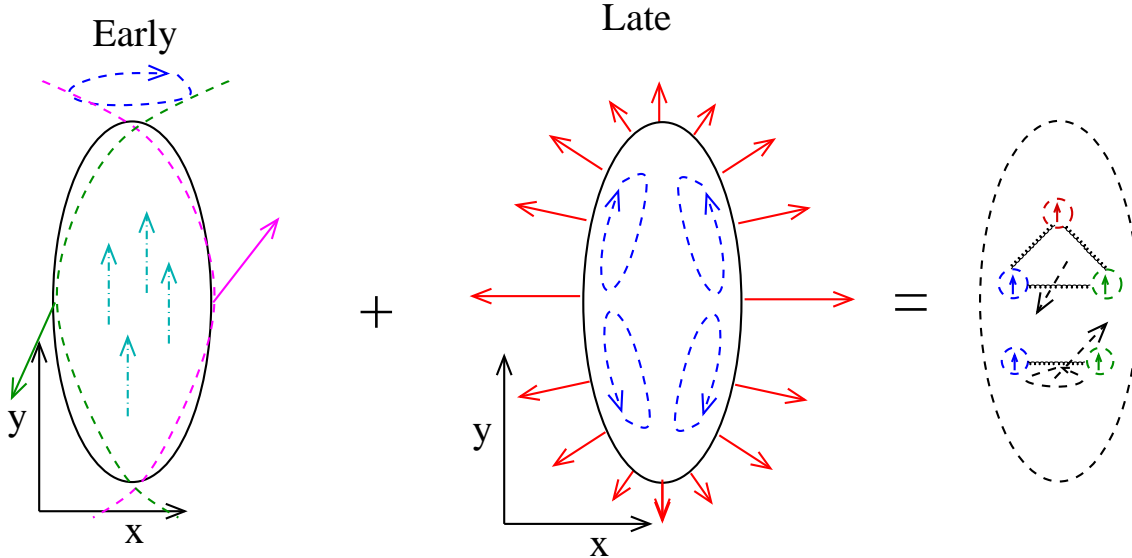


FIG. 1. A schematic representation of the two vorticities in an event with finite impact parameter, together with the expected hadron structure at freeze-out from a coalescence type picture. The impact parameter and beam direction are the x and z directions, respectively.

Here, $f_2^{\mu\nu}$ denotes a symmetric massive spin-2 field. The invariant matrix element and the decay width are computed as below.

$$\mathcal{M} = \frac{g_{f_2\pi\pi}}{m_{f_2}} (p_1 - p_2)_\mu (p_1 - p_2)_\nu \epsilon^{\mu\nu}(\mathbf{p}, \lambda),$$

$$\Gamma = \frac{1}{8\pi} \frac{|p_1|}{m_{f_2}^2} \frac{1}{5} \frac{g_{f_2\pi\pi}^2}{m_{f_2}^2} \frac{32}{3} |p_1|^4 = 185.8 \times (0.843) \text{ MeV}, \quad (7)$$

$$|p_1| = \frac{1}{2} \sqrt{m_{f_2}^2 - 4m_\pi^2} = 623 \text{ MeV}.$$

λ stands for the helicity of f_2 . In f_2 rest frame where helicity is ill defined, it is defined to be a spin projection on z -axis, which depends on our choice of convention. The decay width, the branching ratio(number inside the parentheses) and the masses of the particles are adopted from [21]. The dimensionless coupling constant is obtained to be $g_{f_2\pi\pi} = 5.89$.

Now we compute the general angular distribution $W(\theta, \phi, \rho_{ij})$ of produced pions in $f_2 \rightarrow \pi + \pi$ using phenomenological Lagrangian and helicity formalism in the rest frame of f_2 meson.

A. Phenomenological Lagrangian

Let us assume that initial f_2 is a superposition of different angular momentum states with respective amplitude a_λ . The matrix element of $f_2 \rightarrow \pi + \pi$ in Eq. (7) is generalized as

$$\mathcal{M} = \frac{4g_{f_2\pi\pi}}{m_{f_2}} p_{1\mu} p_{1\alpha} \sum_{\lambda=-2}^2 a_\lambda \epsilon^{\mu\alpha}(\mathbf{p}, \lambda), \quad \rho_{\lambda\lambda'} = a_\lambda a_{\lambda'}^*. \quad (8)$$

We have used that $p_\mu \epsilon^{\mu\alpha}(\mathbf{p}, \lambda) = 0$. $\rho_{\lambda\lambda'}$ is the matrix element of a spin density operator. $W(\theta, \phi, \rho_{ij})$ can be obtained by taking a square of the matrix element in Eq. (8), which is given in Appendix A 1.

$$W(\theta, \phi, \rho_{ij}) = \frac{1}{\Gamma} \frac{1}{32\pi^2} \frac{|p_1|}{m_{f_2}^2} |\mathcal{M}|^2. \quad (9)$$

Γ and $|p_1|$ are given in Eq. (7). The result is same as given in Eq. (A7) obtained in the following subsection using the helicity formalism.

B. Helicity formalism

In 2-body decay, the initial particle is represented by an angular momentum eigenstate at rest $|JM\rangle$. Here J and M are total spin and its projection on the initial quantization axis. On the other hand, the final particle state is given as a simultaneous eigenstate of momentum and helicity, $|ps\lambda\rangle$ in which \mathbf{p} , s and λ stand for the momentum, spin and helicity of a final particle, respectively. The final particle angular distribution is evaluated in the rest frame of the initial particle. Let the final particle momentum be written in terms of the spherical coordinate (p, θ, ϕ) , where θ is the polar angle between the final particle momentum and the initial quantization axis and ϕ is an azimuthal angle.

The helicity rest frame of a final particle is reached by a Lorentz boost along a z -axis, which is followed by a rotation

parametrized by Euler angle of $(\phi, \theta, 0)$. The helicity Lorentz transformation is illustrated in Fig. 2.

We assume that the spin and helicity of the first and second final particles are (s_1, λ_1) and (s_2, λ_2) , respectively. The formula for the normalized angular distribution of a final particle is given in [22].

$$W(\theta, \phi, \rho_{ij}) = \sum_{\lambda_1 \lambda_2} \sum_{MM'} \frac{2J+1}{4\pi} \left| F_{\lambda_1 \lambda_2}^J \right|^2 \times D^{J\dagger}(\phi, \theta, 0) {}^{\lambda} M \rho_{MM'} D^J(\phi, \theta, 0) {}^{M'} {}_{\lambda} \quad (10)$$

$$\sum_{\lambda_1 \lambda_2} \left| F_{\lambda_1 \lambda_2}^J \right|^2 = 1 .$$

Here, $\rho_{MM'}$ stands for the spin-density matrix of the initial particle. $D^J(\phi, \theta, 0)$ is the Wigner D-matrix where $\lambda = \lambda_1 - \lambda_2$ is the difference of helicity of final particles. $F_{\lambda_1 \lambda_2}^J$ is the reduced helicity amplitude. For the decay J into two spin-0 particles, the final particles satisfy $\lambda_1 = \lambda_2 = 0$. In this case, the angular distribution $W(\theta, \phi, \rho_{ij})$ can be written in terms of the spherical harmonics as:

$$W(\theta, \phi, \rho_{ij}) = \sum_{MM'} Y_J^M(\theta, \phi) Y_J^{M'*}(\theta, \phi) \rho_{MM'} . \quad (11)$$

The general angular distribution of produced pion is given in Appendix A, Eq.(A7) as a function of θ, ϕ and spin density matrix element of f_2 meson. After integrating over ϕ , we obtain $W(\theta, \rho_{ii})$ as below.

$$W(\theta, \rho_{ii}) = \frac{5}{16} \left(2\rho_{00} + 3(\rho_{22} + \rho_{-2-2}) + 2(-6\rho_{00} + 6(\rho_{11} + \rho_{-1-1}) - 3(\rho_{22} + \rho_{-2-2})) \cos^2 \theta \right. \\ \left. + 3(6\rho_{00} - 4(\rho_{11} + \rho_{-1-1}) + \rho_{22} + \rho_{-2-2}) \cos^4 \theta \right) . \quad (12)$$

Note, $\rho_{22} + \rho_{11} + \rho_{00} + \rho_{-1-1} + \rho_{-2-2} = 1$.

III. THE BLAST WAVE MODEL

We proceed with our calculation of the spin density matrix element of f_2 in the medium created in heavy-ion collisions, where we can neglect baryon number density. To describe the medium we will use a simplified model, developed in [14, 15] in which the transverse component of the fluid follows an elliptical expansion, while the longitudinal component is assumed to be boost-invariant. The elliptical parameterization of the region created in this interaction in the $x - y$ plane allows us to consider the effects of elliptic flow, which is described by the following expressions [14]:

$$x = r_{\max} \sqrt{1-\epsilon} \cos \phi_r, \\ y = r_{\max} \sqrt{1+\epsilon} \sin \phi_r, \quad (13)$$

where ϵ (spatial size deformation) and r_{\max} (transverse size) are model parameters and ϕ_r is azimuthal angle in the transverse plane. The flow velocity is defined by:

$$u^\mu = \left(\frac{t}{N}, \frac{x}{N} \sqrt{1+\delta}, \frac{y}{N} \sqrt{1-\delta}, \frac{z}{N} \right), \quad (14)$$

δ is the parameter that accounts for the anisotropy of the transverse flow, and N is a normalization parameter given by:

$$N = \sqrt{\tau^2 - (x^2 - y^2)\delta} \quad , \quad \tau^2 = t^2 - x^2 - y^2 - z^2, \quad (15)$$

where the spatial component z is

$$z = \sqrt{\tau_f^2 + x^2 + y^2} \sinh \eta. \quad (16)$$

η is space-time rapidity and τ_f is lifetime of a system. At this point, we can determine the thermal vorticity:

$$\Omega_{\mu, \nu} = -\frac{1}{2T} (\partial_\mu u_\nu - \partial_\nu u_\mu) - \frac{1}{2T^2} (u_\mu \partial_\nu T - u_\nu \partial_\mu T). \quad (17)$$

It was shown in [14] that the first and second terms on the right-hand side of Eq. (17) are equal, using the relativistic hydrodynamic equations at zero baryon density. The spatial components of the thermal vorticity, where $i, j, k = 1, 2, 3$, are defined as:

$$\Omega_i = \frac{1}{2} \epsilon_{ijk} \Omega_{jk}, \quad (18)$$

where its values are given explicitly:

$$\Omega_1 = \frac{yz}{TN^3} \left(1 - \delta - \sqrt{1-\delta} \right), \\ \Omega_2 = \frac{zx}{TN^3} \left(\sqrt{1+\delta} - 1 - \delta \right), \\ \Omega_3 = \frac{xy\sqrt{1-\delta^2}}{TN^3} \left(\sqrt{1+\delta} - \sqrt{1-\delta} \right). \quad (19)$$

While the model in [13] does not have global polarization ([13] added it at the *quark level*), it can easily be added by

$$\Omega_2(x, y, z) \rightarrow \Omega_2(x, y, z) + \Omega_{\text{global}}. \quad (20)$$

where Ω_{global} is a constant throughout the event, whose numerical estimate is approximately given in the introduction of [16] as $0.02 \text{ fm}^{-1} \rightarrow 0.00394 \text{ GeV}$, therefore we have $\Omega_{\text{global}} \rightarrow \Omega_{\text{global}}/T = 0.024$ where $T = 0.165 \text{ GeV} \rightarrow 0.837 \text{ fm}^{-1}$.

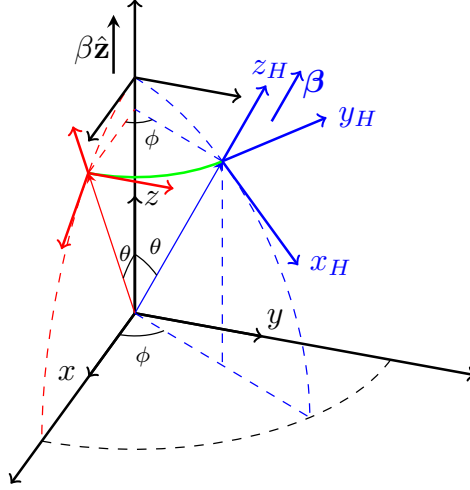


FIG. 2. Helicity Lorentz transformation of a particle. Subscript H denotes the helicity rest frame.

TABLE I. Thermal model parameters used in our calculation [14, 15].

c%	ϵ	δ	τ_f (fm)	r_{\max} (fm)
0-15	0.055	0.12	7.666	6.540
15-30	0.097	0.26	6.258	5.417
30-60	0.137	0.37	4.266	3.779

IV. RESULTS AND DISCUSSION

In this section, we present our results for the diagonal elements of the f_2 spin density matrix, as well as the real and imaginary parts of ρ_{20} , computed from Eq. (1) within the blast-wave model. The density matrix elements are expressed in terms of the spatial components of the thermal vorticity and the temperature; the explicit expressions for the alignment factors are provided in Appendix B. We evaluated the mean values of diagonal elements by averaging over spacetime rapidity range $-4 \leq \eta \leq 4$ for three different centrality classes (0-15%, 15-30%, and 30-60%). The results are shown in Figs. 3, 4 and 5, which correspond to $\Omega_{\text{global}} = 0$, $\Omega_{\text{global}} = 0.024$ and $\Omega_{\text{global}} = 1.2$, respectively. The mean values of real and imaginary part of ρ_{20} were also obtained in the same manner and are shown in Fig. 6. The parameters used for our calculations are listed in Table I.

The oscillatory behavior of the density matrix element becomes distinct in more peripheral collisions, as they induce larger vorticity than head-on collisions. We also note that the addition of global vorticity perpendicular to the reaction plane increases the amplitude of ρ_{00} .

By symmetry, since in equilibrium there is only one angular momentum vector, observable combinations (Eq. (A7)) involving $\rho_{\pm 2, \pm 1}$ and $\rho_{\pm 1, 0}$ matrix elements are odd about this vector, and hence will be zero when integrated over the ϕ_r angle. Thus, comparing Eq. (A7) with Fig. 6 all observ-

able combinations of the type $\rho_{|i| \neq |j|}$ elements are zero except $\rho_{2,0}$ (Shown in Fig 6). This is however not true if spin and vorticity are not in equilibrium, i.e. scenarios such as [8–10], in which case the axial symmetry is broken and all density matrix elements are potentially non-zero. $\rho_{|i| \neq |j|}$ density matrix elements are therefore good candidates for signatures for spin-vorticity at non-equilibrium and a dynamics such as Eq. (2). Estimates of the mixing, $1 - \text{Tr} \rho^2$ might also be used to rule out the statistical model considered here since it predicts a maximally mixed state. However, since we do not have access to all density matrix elements, the mixing will at best be a broad confidence region.

While in this work we focused on the spin-0 decay of f_2 mesons, the recently measured χ_c spin-2 state decay into fermions [23] could also be used for a similar analysis, although of course the angular dependence and its relation to vorticity is expected to be different.

In conclusion, in this work we have shown that the density matrix structure of the f_2 meson decay into scalars is both rich in physics and experimentally accessible, which makes it a very promising probe of vorticity and spin dynamics in heavy ion collisions. We look forward to further experimental and phenomenological developments in this direction.

ACKNOWLEDGMENTS

The work of I. Park, G. Torrieri and S.H. Lee were supported by the Korean-Brazilian collaboration fund by the Korea National Research Foundation (NRF) under Grant No. RS-2023-NR121103. B. Kim and S. Lim acknowledge support from the National Research Foundation of Korea (NRF) grant funded by the Korean government (MSIT) under Contract No. NRF-2008-00458.

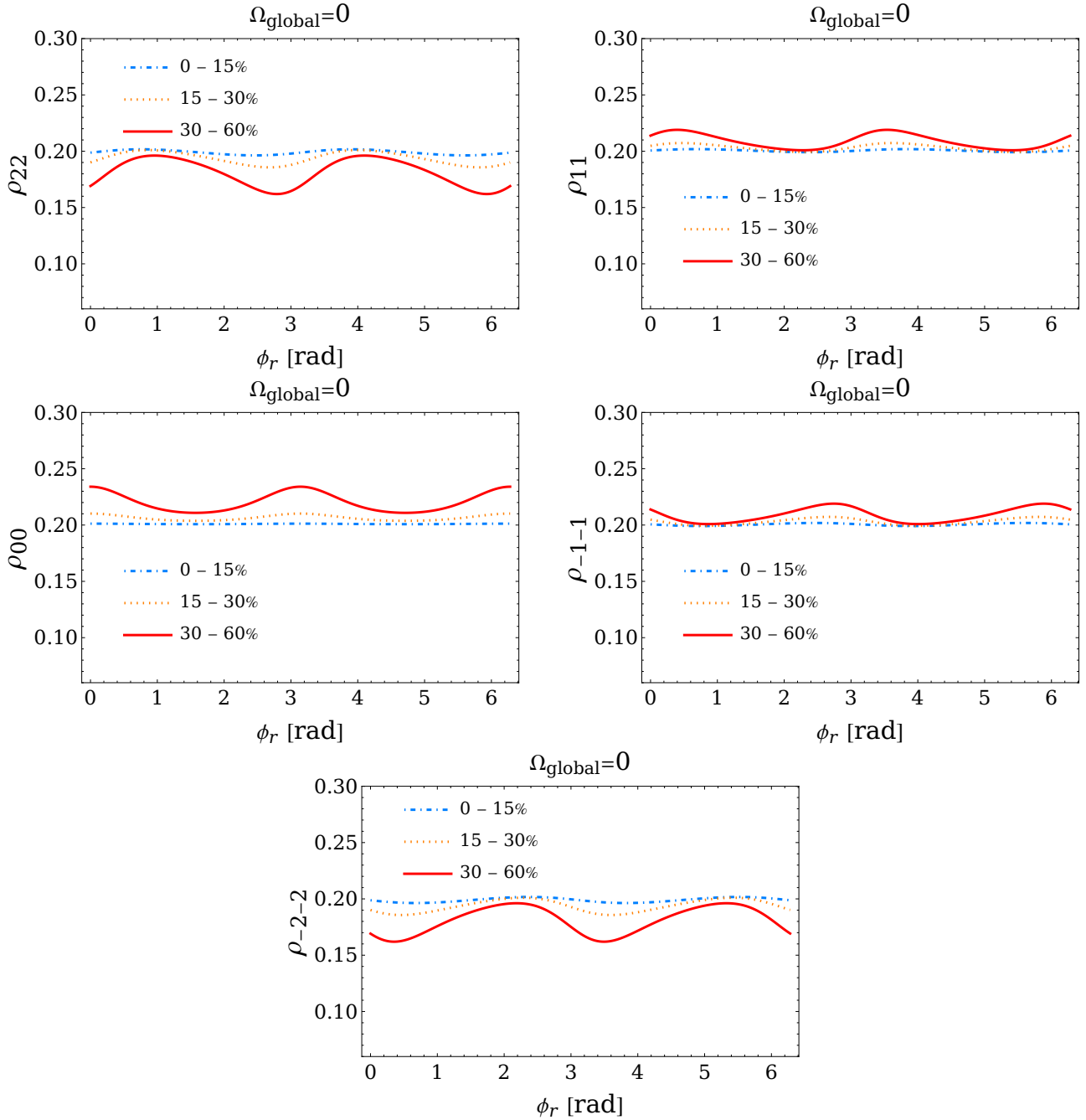


FIG. 3. Diagonal density matrix elements for various event centrality classes computed assuming thermal production (Eq. (1)) as a function of the angle w.r.t. impact parameter, assuming the blast wave picture with elliptic flow and polarization , [14, 15] and no global vorticity .

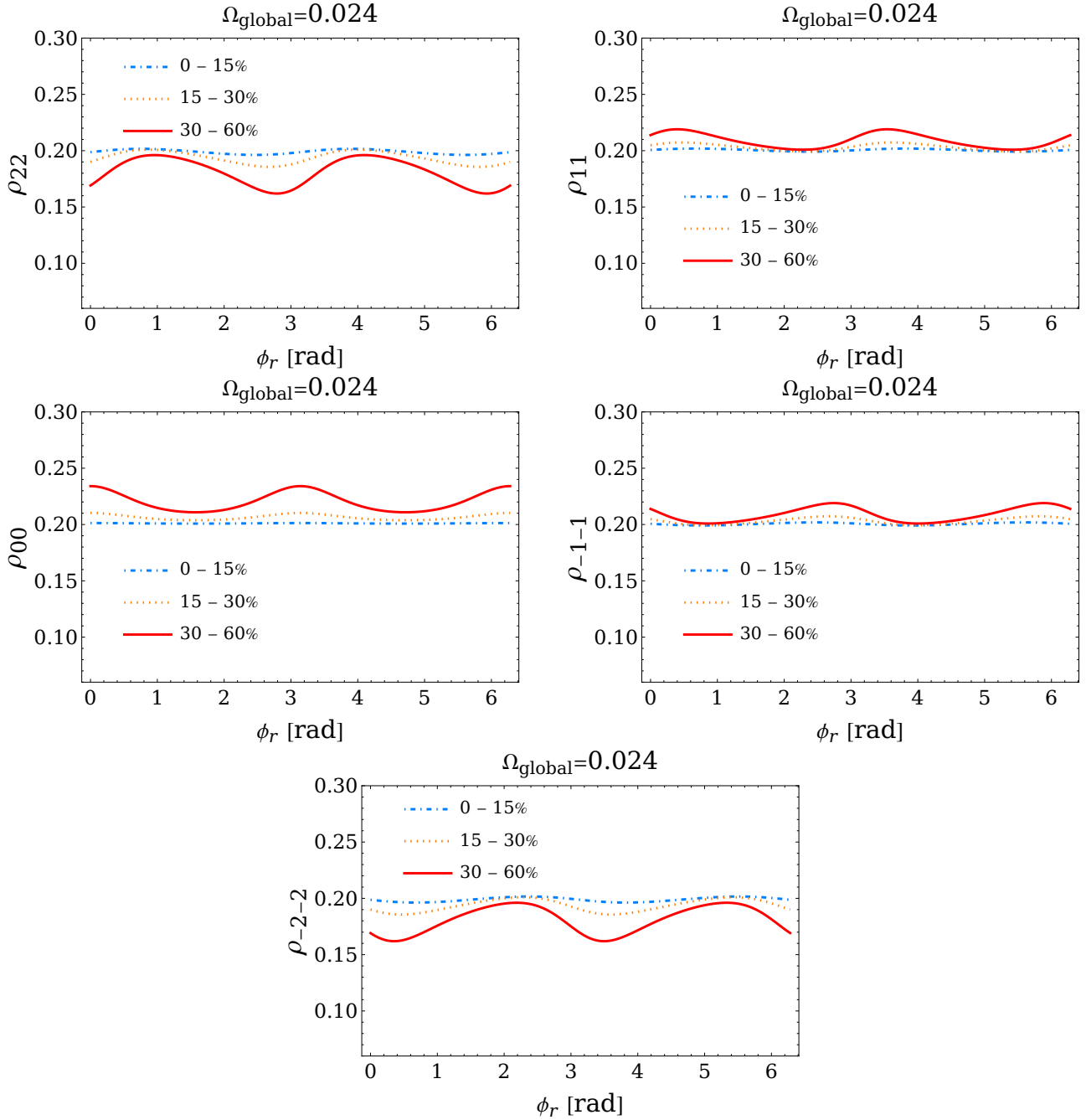


FIG. 4. Diagonal density matrix elements for various centrality classes, computed assuming thermal production (Eq. (1)) as a function of the angle w.r.t. impact parameter, assuming the blast wave picture with elliptic flow and polarization , [14, 15] as well as a global vorticity of [16].

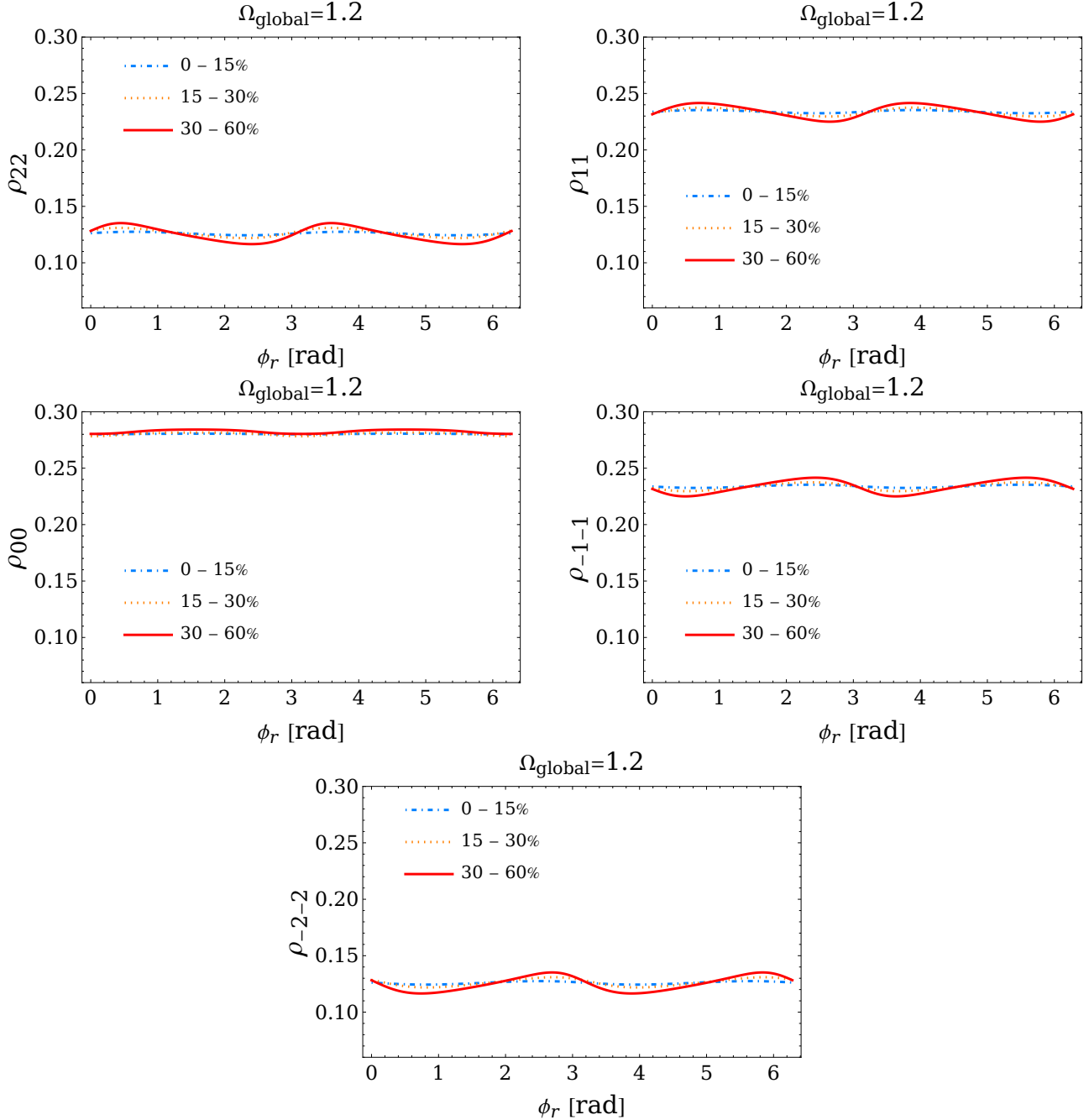


FIG. 5. Diagonal density matrix elements for various centrality classes, computed assuming thermal production (Eq. (1)) as a function of the angle w.r.t. impact parameter, assuming the blast wave picture with elliptic flow and polarization , [14, 15] as well as a global vorticity of [16] multiplied by a factor of 50 .

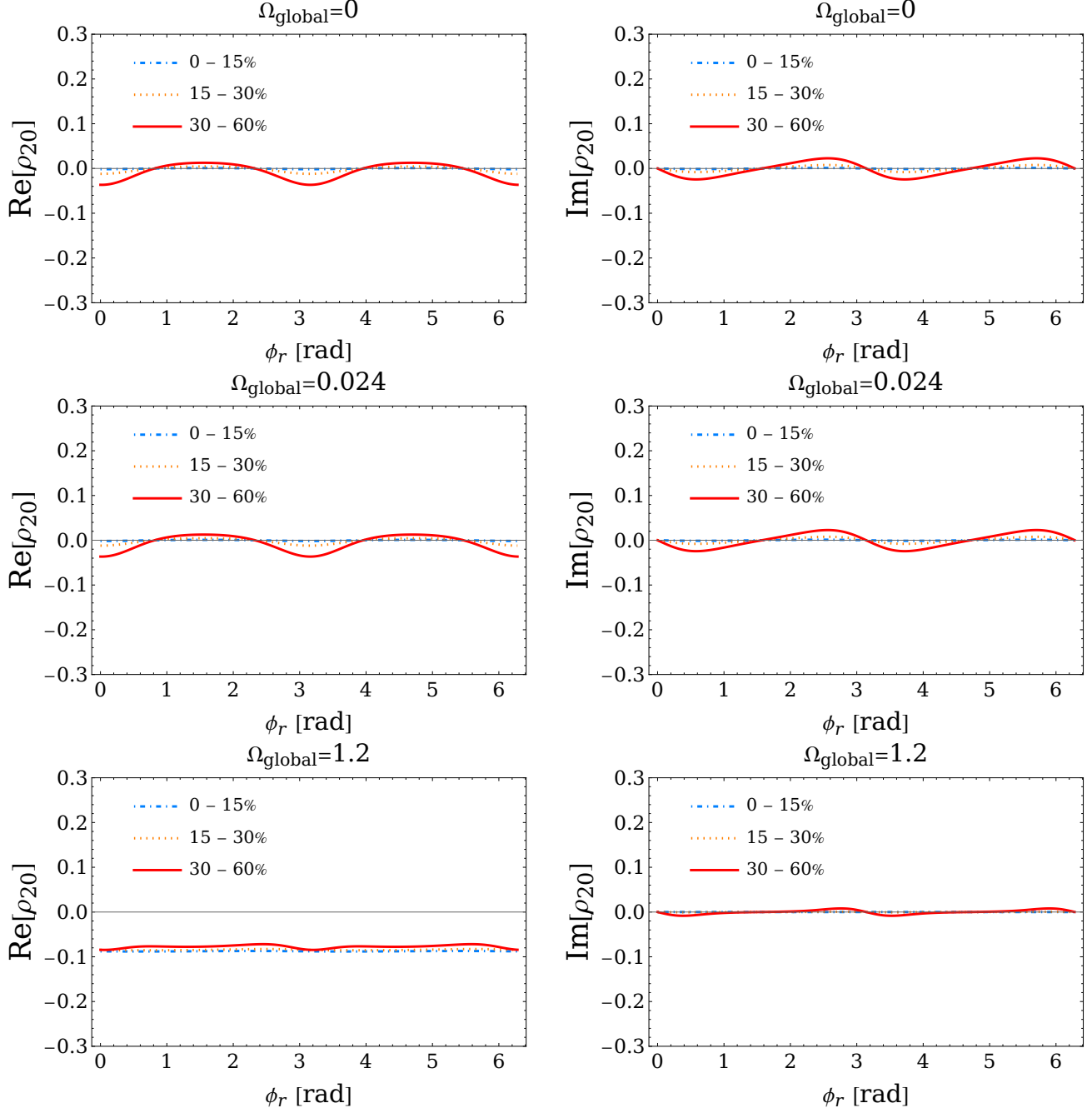


FIG. 6. Non-zero $\rho_{|i| \neq |j|}$ matrix elements for zero and finite vorticity. $\rho_{0,-j}$ are the same as $\rho_{0,j}$ by symmetry. All other $\rho_{|i| \neq |j|}$ components of the density matrix, averaged over the space-time rapidity, were found to be zero.

Appendix A: Calculation of general angular distribution of $f_2(1270) \rightarrow \pi + \pi$

1. Interaction Lagrangian

The polarization tensor of a massive spin-2 particle is obtained through a direct product between spin-1 polarization vectors. The Clebsch-Gordan(CG) coefficient has been taken from [21].

$$\begin{aligned} \epsilon^{\mu\nu}(\mathbf{0}, \pm 2) &= \epsilon^\mu(\mathbf{0}, \pm 1)\epsilon^\nu(\mathbf{0}, \pm 1) - \frac{1}{2} \begin{pmatrix} 0 & 0 & 0 & 0 \\ 0 & 1 & \pm i & 0 \\ 0 & \pm i & -1 & 0 \\ 0 & 0 & 0 & 0 \end{pmatrix}, \\ \epsilon^{\mu\nu}(\mathbf{0}, \pm 1) &= \frac{1}{\sqrt{2}} (\epsilon^\mu(\mathbf{0}, \pm 1)\epsilon^\nu(\mathbf{0}, 0) + \epsilon^\mu(\mathbf{0}, 0)\epsilon^\nu(\mathbf{0}, \pm 1)) = \frac{1}{2} \begin{pmatrix} 0 & 0 & 0 & 0 \\ 0 & 0 & 0 & \mp 1 \\ 0 & 0 & 0 & -i \\ 0 & \mp 1 & -i & 0 \end{pmatrix}, \\ \epsilon^{\mu\nu}(\mathbf{0}, 0) &= \frac{1}{\sqrt{6}} (\epsilon^\mu(\mathbf{0}, +1)\epsilon^\nu(\mathbf{0}, -1) + \epsilon^\mu(\mathbf{0}, -1)\epsilon^\nu(\mathbf{0}, +1)) + \sqrt{\frac{2}{3}} \epsilon^\mu(\mathbf{0}, 0)\epsilon^\nu(\mathbf{0}, 0) = \frac{1}{\sqrt{6}} \begin{pmatrix} 0 & 0 & 0 & 0 \\ 0 & -1 & 0 & 0 \\ 0 & 0 & -1 & 0 \\ 0 & 0 & 0 & 2 \end{pmatrix}. \end{aligned} \quad (\text{A1})$$

The completeness relationship of spin-2 polarization tensor is given in [24, 25].

$$\begin{aligned} \sum_{\lambda=-2}^2 \epsilon^{\mu\alpha}(\mathbf{p}, \lambda)\epsilon^{\nu\beta*}(\mathbf{p}, \lambda) &= \Delta^{\mu\nu\alpha\beta}(2, \mathbf{p}) = \frac{1}{2} (I^{\mu\nu}I^{\alpha\beta} + I^{\mu\beta}I^{\nu\alpha}) - \frac{1}{3} I^{\mu\alpha}I^{\nu\beta}, \\ I^{\mu\nu} &= -g^{\mu\nu} + \frac{p^\mu p^\nu}{p^2}, \\ \epsilon^{\mu\nu}(\mathbf{p}, \lambda) &= \epsilon^{\nu\mu}(\mathbf{p}, \lambda), \quad p_\mu\epsilon^{\mu\nu}(\mathbf{p}, \lambda) = 0. \end{aligned} \quad (\text{A2})$$

Assume that the final pion momentum in f_2 rest frame is parameterized by $(|\mathbf{p}_1|, \theta, \phi)$ where θ and ϕ are polar and azimuthal angle with respect to the initial quantization axis. $|\mathbf{p}_1|$ is given in Eq. (7).

$$\mathbf{p}_1^\mu = (\sqrt{|\mathbf{p}_1|^2 + m_\pi^2}, |\mathbf{p}_1|\sin\theta\cos\phi, |\mathbf{p}_1|\sin\theta\sin\phi, |\mathbf{p}_1|\cos\theta). \quad (\text{A3})$$

The squared of matrix element in Eq. (8) is calculated to be

$$|\mathcal{M}|^2 = \frac{128\pi g_{f_2\pi\pi}^2}{15m_{f_2}^2} |\mathbf{p}_1|^4 W(\theta, \phi, \rho_{ij}). \quad (\text{A4})$$

$W(\theta, \phi, \rho_{ij})$ is given in the next subsection.

2. Helicity formalism

The rotation in 3D space can be parameterized by Euler angles, (α, β, γ) . We make a rotation around a fixed z -axis by an angle of γ followed by a rotation around a fixed y -axis by an angle of β finally followed by a rotation around a fixed z -axis by an angle of α . The Wigner D-matrix is defined as below,

$$D^J(\alpha, \beta, \gamma)_{MM'} = \langle JM | U(R(\alpha, \beta, \gamma)) | JM' \rangle = e^{-i(M\alpha + M'\gamma)} d^J(\beta)_{MM'}. \quad (\text{A5})$$

More information about helicity formalism can be found in [22, 26, 27]. The angular distribution given in Eq. (10) can be rewritten in terms of trigonometric function as below,

$$\begin{aligned} W(\theta, \phi, \rho_{ij}) &= \sum_{\lambda_1 \lambda_2} \sum_{MM'} \frac{2J+1}{4\pi} d^J(\theta)_{M\lambda} d^J(\theta)_{M'\lambda} \left| F_{\lambda_1 \lambda_2}^J \right|^2 \\ &\times (\text{Re}[\rho_{MM'}] \cos(M - M')\phi - \text{Im}[\rho_{MM'}] \sin(M - M')\phi). \end{aligned} \quad (\text{A6})$$

As a result, the distribution of final pion produced in $f_2 \rightarrow \pi + \pi$ is obtained by inserting $J = 2$ in Eq. (10) or Eq. (11).

$$\begin{aligned}
W(\theta, \phi, \rho_{ij}) = & \frac{5}{64\pi} \left(\rho_{00} (3 \cos 2\theta + 1)^2 + 6(\rho_{11} + \rho_{-1-1}) \sin^2 2\theta + 6(\rho_{22} + \rho_{-2-2}) \sin^4 \theta \right. \\
& - 4\sqrt{6} \sin 2\theta (3 \cos^2 \theta - 1) (\operatorname{Re}[\rho_{10} - \rho_{0-1}] \cos \phi - \operatorname{Im}[\rho_{10} - \rho_{0-1}] \sin \phi) \\
& - 12 \sin 2\theta \sin^2 \theta (\operatorname{Re}[\rho_{21} - \rho_{-1-2}] \cos \phi - \operatorname{Im}[\rho_{21} - \rho_{-1-2}] \sin \phi) \\
& + \sqrt{6} (3 \sin^2 2\theta - 4 \sin^2 \theta) (\operatorname{Re}[\rho_{20} + \rho_{0-2}] \cos 2\phi - \operatorname{Im}[\rho_{20} + \rho_{0-2}] \sin 2\phi) \\
& - 12 \sin^2 2\theta (\operatorname{Re}[\rho_{1-1}] \cos 2\phi - \operatorname{Im}[\rho_{1-1}] \sin 2\phi) \\
& + 12 \sin 2\theta \sin^2 \theta (\operatorname{Re}[\rho_{2-1} - \rho_{1-2}] \cos 3\phi - \operatorname{Im}[\rho_{2-1} - \rho_{1-2}] \sin 3\phi) \\
& \left. + 12 \sin^4 \theta (\operatorname{Re}[\rho_{2-2}] \cos 4\phi - \operatorname{Im}[\rho_{2-2}] \sin 4\phi) \right). \tag{A7}
\end{aligned}$$

The integration over azimuthal angle ϕ of the angular distribution given in Eq. (11) yields the distribution in terms of polar angle θ and diagonal spin density matrix elements.

$$\begin{aligned}
W(\theta, \rho_{ii}) = & \frac{5}{12} \left(\rho_{11} + \rho_{-1-1} + 2(\rho_{22} + \rho_{-2-2}) + 3(\rho_{11} + \rho_{-1-1} - \rho_{22} - \rho_{-2-2}) P_1(\cos \theta)^2 \right. \\
& \left. + (\rho_{22} + \rho_{-2-2} - 4(\rho_{11} + \rho_{-1-1}) + 6\rho_{00}) P_2(\cos \theta)^2 \right). \tag{A8}
\end{aligned}$$

$P_J(\cos \theta)$ is Legendre polynomial. The formula in terms of $\cos \theta$ is given in Eq. (12).

Appendix B: Diagonal density matrix components for the f_2 tensor meson

Using the density matrix definition of the f_2 tensor meson in Eq. (1), and assuming local thermodynamic equilibrium, we can explicitly obtain all diagonal elements of its density matrix, where the Pauli matrix for $S = 2$ are:

$$S_x = \begin{pmatrix} 0 & 1 & 0 & 0 & 0 \\ 1 & 0 & \sqrt{\frac{3}{2}} & 0 & 0 \\ 0 & \sqrt{\frac{3}{2}} & 0 & \sqrt{\frac{3}{2}} & 0 \\ 0 & 0 & \sqrt{\frac{3}{2}} & 0 & 1 \\ 0 & 0 & 0 & 1 & 0 \end{pmatrix}, \quad S_y = \begin{pmatrix} 0 & -i & 0 & 0 & 0 \\ i & 0 & -i\sqrt{\frac{3}{2}} & 0 & 0 \\ 0 & i\sqrt{\frac{3}{2}} & 0 & -i\sqrt{\frac{3}{2}} & 0 \\ 0 & 0 & i\sqrt{\frac{3}{2}} & 0 & -i \\ 0 & 0 & 0 & i & 0 \end{pmatrix}, \quad S_z = \begin{pmatrix} 2 & 0 & 0 & 0 & 0 \\ 0 & 1 & 0 & 0 & 0 \\ 0 & 0 & 0 & 0 & 0 \\ 0 & 0 & 0 & -1 & 0 \\ 0 & 0 & 0 & 0 & -2 \end{pmatrix}. \tag{B1}$$

From the definition of the spatial components of thermal vorticity Eq.(18) (it is important to note that $\frac{\vec{\Omega}}{T} \rightarrow \vec{\Omega}$ in order to maintain consistency with the definition of thermal vorticity) together of density matrix Eq. (1) and Pauli matrix to $S = 2$, Eq. (B1) we can obtain the trace of density matrix:

$$\Omega = \sqrt{\Omega_1^2 + \Omega_2^2 + \Omega_3^2}, \tag{B2}$$

$$\operatorname{Tr}(\rho) = Z = 1 + 2 \cosh(\Omega) + 2 \cosh(2\Omega). \tag{B3}$$

The coefficient: $\rho_{\pm 2\pm 2}(\Omega_1, \Omega_2, \Omega_3, T)$:

$$\begin{aligned}
\rho_{\pm 2\pm 2}(\Omega_1, \Omega_2, \Omega_3, T) = & \frac{1}{Z\Omega^4} \left(\Omega_1^4 \cosh^4 \left(\frac{\Omega}{2} \right) + \Omega_2^4 \cosh^4 \left(\frac{\Omega}{2} \right) + \Omega_1^2 \cosh^2 \left(\frac{\Omega}{2} \right) (\Omega_2^2 - 2\Omega_3^2 \pm 2\Omega_3 \Omega \sinh(\Omega) + \right. \\
& \left. + (\Omega_2^2 + 4\Omega_3^2) \cosh(\Omega)) + 2\Omega_2^2 \Omega_3 \cosh^2 \left(\frac{\Omega}{2} \right) (\Omega_3 (2 \cosh(\Omega) - 1) \pm \Omega \sinh(\Omega)) + \Omega_3^3 (\Omega_3 \cosh(2\Omega) \pm \Omega \sinh(2\Omega)) \right). \tag{B4}
\end{aligned}$$

The coefficient: $\rho_{\pm 1\pm 1}(\Omega_1, \Omega_2, \Omega_3, T)$:

$$\begin{aligned}
\rho_{\pm 1\pm 1}(\Omega_1, \Omega_2, \Omega_3, T) = & \frac{1}{2Z\Omega^4} \left((\Omega_3^2 + (\Omega_1^2 + \Omega_2^2) (2 \cosh(\Omega) - 1)) (\Omega_1^2 + \Omega_2^2 \pm 2\Omega_3 \Omega \sinh(\Omega) + \right. \\
& \left. + (\Omega_1^2 + \Omega_2^2 + 2\Omega_3^2) \cosh(\Omega)) \right). \tag{B5}
\end{aligned}$$

The coefficient: $\rho_{00}(\Omega_1, \Omega_2, \Omega_3, T)$:

$$\rho_{00}(\Omega_1, \Omega_2, \Omega_3, T) = \frac{1}{4Z\Omega^4} \left(3(\Omega_1^2 + \Omega_2^2)^2 \cosh(2\Omega) + 12\Omega_3^2(\Omega_1^2 + \Omega_2^2) \cosh(\Omega) + (\Omega_1^2 + \Omega_2^2 - 2\Omega_3^2)^2 \right). \quad (\text{B6})$$

The coefficient: $\text{Re}[\rho_{10} - \rho_{0-1}]$:

$$\text{Re}[\rho_{10} - \rho_{0-1}] = \frac{2\sqrt{6}\Omega_1\Omega_3 \sinh^2\left(\frac{\Omega}{2}\right) (\Omega_3^2 + (\Omega_1^2 + \Omega_2^2) \cosh(\Omega))}{Z\Omega^4} \quad (\text{B7})$$

The coefficient: $\text{Im}[\rho_{10} - \rho_{0-1}]$:

$$\text{Im}[\rho_{10} - \rho_{0-1}] = -\frac{2\sqrt{6}\Omega_2\Omega_3 \sinh^2\left(\frac{\Omega}{2}\right) (\Omega_3^2 + (\Omega_1^2 + \Omega_2^2) \cosh(\Omega))}{Z\Omega^4}. \quad (\text{B8})$$

The coefficient: $\text{Re}[\rho_{21} - \rho_{-1-2}]$:

$$\text{Re}[\rho_{21} - \rho_{-1-2}] = \frac{2\Omega_1\Omega_3 \sinh^2\left(\frac{\Omega}{2}\right) (3\Omega_1^2 + 3\Omega_2^2 + 2\Omega_3^2 + (4\Omega_3^2 + 3(\Omega_1^2 + \Omega_2^2)) \cosh(\Omega))}{Z\Omega^4}. \quad (\text{B9})$$

The coefficient: $\text{Im}[\rho_{21} - \rho_{-1-2}]$:

$$\text{Im}[\rho_{21} - \rho_{-1-2}] = \frac{2\Omega_2\Omega_3 \sinh^2\left(\frac{\Omega}{2}\right) (-3\Omega_1^2 - 3\Omega_2^2 - 2\Omega_3^2 - (4\Omega_3^2 + 3(\Omega_1^2 + \Omega_2^2)) \cosh(\Omega))}{Z\Omega^4}. \quad (\text{B10})$$

The coefficient: $\text{Re}[\rho_{20} + \rho_{0-2}]$:

$$\text{Re}[\rho_{20} + \rho_{0-2}] = \frac{\sqrt{6}(\Omega_1^2 - \Omega_2^2) \sinh^2\left(\frac{\Omega}{2}\right) (\Omega_1^2 + \Omega_2^2 + (\Omega_1^2 + \Omega_2^2 + 2\Omega_3^2) \cosh(\Omega))}{Z\Omega^4}. \quad (\text{B11})$$

The coefficient: $\text{Im}[\rho_{20} + \rho_{0-2}]$:

$$\text{Im}[\rho_{20} + \rho_{0-2}] = -\frac{2\sqrt{6}\Omega_1\Omega_2 \sinh^2\left(\frac{\Omega}{2}\right) (\Omega_1^2 + \Omega_2^2 + (\Omega_1^2 + \Omega_2^2 + 2\Omega_3^2) \cosh(\Omega))}{Z\Omega^4}. \quad (\text{B12})$$

The coefficient: $\text{Re}[\rho_{1-1}]$:

$$\text{Re}[\rho_{1-1}] = \frac{(\Omega_1^2 - \Omega_2^2) \sinh^2\left(\frac{\Omega}{2}\right) (3\Omega_3^2 + (\Omega_1^2 + \Omega_2^2) (2 \cosh(\Omega) + 1))}{Z\Omega^4}. \quad (\text{B13})$$

The coefficient: $\text{Im}[\rho_{1-1}]$:

$$\text{Im}[\rho_{1-1}] = -\frac{2\Omega_1\Omega_2 \sinh^2\left(\frac{\Omega}{2}\right) (3\Omega_3^2 + (\Omega_1^2 + \Omega_2^2) (2 \cosh(\Omega) + 1))}{Z\Omega^4}. \quad (\text{B14})$$

The coefficient: $\text{Re}[\rho_{2-1} - \rho_{1-2}]$:

$$\text{Re}[\rho_{2-1} - \rho_{1-2}] = \frac{4\Omega_1(\Omega_1^2 - 3\Omega_2^2)\Omega_3 \sinh^4\left(\frac{\Omega}{2}\right)}{Z\Omega^4}. \quad (\text{B15})$$

The coefficient: $\text{Im}[\rho_{2-1} - \rho_{1-2}]$:

$$\text{Im}[\rho_{2-1} - \rho_{1-2}] = \frac{4\Omega_2(\Omega_2^2 - 3\Omega_1^2)\Omega_3 \sinh^4\left(\frac{\Omega}{2}\right)}{Z\Omega^4}. \quad (\text{B16})$$

The coefficient: $\text{Re}[\rho_{2-2}]$:

$$\text{Re}[\rho_{2-2}] = \frac{(\Omega_1^4 - 6\Omega_2^2\Omega_1^2 + \Omega_2^4) \sinh^4\left(\frac{\Omega}{2}\right)}{Z\Omega^4}. \quad (\text{B17})$$

The coefficient: $\text{Im}[\rho_{2-2}]$:

$$\text{Im}[\rho_{2-2}] = \frac{4\Omega_1\Omega_2(\Omega_2^2 - \Omega_1^2)\sinh^4(\frac{\Omega}{2})}{Z\Omega^4}. \quad (\text{B18})$$

We can obtain the mean value of diagonal elements over the space-time rapidity in following way:

$$\langle \rho_{i,j}(\phi_r) \rangle = \frac{1}{\eta - \eta_0} \int_{\eta_0}^{\eta} d\eta' \rho_{i,j}(\phi_r, \eta'), \quad (\text{B19})$$

where $\eta = 4$ and $\eta_0 = -4$.

[1] L. Adamczyk *et al.* (STAR), Global Λ hyperon polarization in nuclear collisions: evidence for the most vortical fluid, *Nature* **548**, 62 (2017), arXiv:1701.06657 [nucl-ex].

[2] X.-L. Xia, H. Li, X.-G. Huang, and H. Zhong Huang, Local spin alignment of vector mesons in relativistic heavy-ion collisions, *Phys. Lett. B* **817**, 136325 (2021), arXiv:2010.01474 [nucl-th].

[3] M. S. Abdallah *et al.* (STAR), Pattern of global spin alignment of ϕ and K^{*0} mesons in heavy-ion collisions, *Nature* **614**, 244 (2023), arXiv:2204.02302 [hep-ph].

[4] S. Acharya *et al.* (ALICE), Evidence of Spin-Orbital Angular Momentum Interactions in Relativistic Heavy-Ion Collisions, *Phys. Rev. Lett.* **125**, 012301 (2020), arXiv:1910.14408 [nucl-ex].

[5] S. Acharya *et al.* (ALICE), First measurement of D^{*+} vector meson spin alignment in Pb–Pb collisions at $\sqrt{s_{\text{NN}}} = 5.02$ TeV, *JHEP* **10**, 094, arXiv:2504.00714 [nucl-ex].

[6] Z.-T. Liang and X.-N. Wang, Spin alignment of vector mesons in non-central A+A collisions, *Phys. Lett. B* **629**, 20 (2005), arXiv:nucl-th/0411101.

[7] D. Montenegro and G. Torrieri, Causality and dissipation in relativistic polarizable fluids, *Phys. Rev. D* **100**, 056011 (2019), arXiv:1807.02796 [hep-th].

[8] D. Montenegro and G. Torrieri, Linear response theory and effective action of relativistic hydrodynamics with spin, *Phys. Rev. D* **102**, 036007 (2020), arXiv:2004.10195 [hep-th].

[9] G. Torrieri and D. Montenegro, Linear response hydrodynamics of a relativistic dissipative fluid with spin, *Phys. Rev. D* **107**, 076010 (2023), arXiv:2207.00537 [hep-th].

[10] D. Montenegro and G. Torrieri, Causality of polarizable dissipative fluids from Lagrangian hydrodynamics, *Phys. Rev. D* **112**, 034041 (2025), arXiv:2506.17327 [nucl-th].

[11] M. Hongo, X.-G. Huang, M. Kaminski, M. Stephanov, and H.-U. Yee, Relativistic spin hydrodynamics with torsion and linear response theory for spin relaxation, *JHEP* **11**, 150, arXiv:2107.14231 [hep-th].

[12] K. J. Gonçalves and G. Torrieri, Spin alignment of vector mesons as a probe of spin hydrodynamics and freeze-out, *Phys. Rev. C* **105**, 034913 (2022), arXiv:2104.12941 [nucl-th].

[13] K. J. Gonçalves, G. Torrieri, and R. Ryblewski, Meson spin alignment and baryon polarization from coalescence with spin-vorticity nonequilibrium, *Phys. Rev. C* **112**, 014901 (2025), arXiv:2410.16448 [hep-ph].

[14] W. Florkowski, A. Kumar, R. Ryblewski, and A. Mazeliauskas, Longitudinal spin polarization in a thermal model, *Phys. Rev. C* **100**, 054907 (2019), arXiv:1904.00002 [nucl-th].

[15] W. Florkowski, A. Kumar, A. Mazeliauskas, and R. Ryblewski, Effect of thermal shear on longitudinal spin polarization in a thermal model, *Phys. Rev. C* **105**, 064901 (2022), arXiv:2112.02799 [hep-ph].

[16] F. Becattini, I. Karpenko, M. Lisa, I. Upsal, and S. Voloshin, Global hyperon polarization at local thermodynamic equilibrium with vorticity, magnetic field and feed-down, *Phys. Rev. C* **95**, 054902 (2017), arXiv:1610.02506 [nucl-th].

[17] A. Khatun (ALICE), UPC physics with ALICE in Run 3, *Phys. Proc. UPC* **1**, 22 (2024), arXiv:2405.19069 [hep-ex].

[18] P. H. De Moura, K. J. Gonçalves, and G. Torrieri, Quarkonium spin alignment in a vortical medium, *Phys. Rev. D* **108**, 034032 (2023), arXiv:2305.02985 [hep-ph].

[19] V. Shklyar, H. Lenske, U. Mosel, and G. Penner, Coupled-channel analysis of the omega-meson production in πN and gamma N reactions for c.m. energies up to 2-GeV, *Phys. Rev. C* **71**, 055206 (2005), [Erratum: *Phys. Rev. C* 72, 019903 (2005)], arXiv:nucl-th/0412029.

[20] M. Suzuki, Tensor meson dominance: Phenomenology of the f_2 meson, *Phys. Rev. D* **47**, 1043 (1993).

[21] S. Navas *et al.* (Particle Data Group), Review of particle physics, *Phys. Rev. D* **110**, 030001 (2024).

[22] E. Leader, *Spin in Particle Physics*, Vol. 15 (Cambridge University Press, 2001).

[23] Study of χ_c production in pPb collisions at $\sqrt{s_{\text{NN}}} = 8.16$ TeV with the CMS experiment (2025).

[24] S.-H. Kim, Y. Oh, S. Son, S. Sakinah, and M.-K. Cheoun, Effective Lagrangian for strong and electromagnetic interactions of high-spin resonances, *Phys. Rev. D* **111**, 054031 (2025), arXiv:2412.18927 [hep-ph].

[25] S. Y. Choi, J. Lee, J. S. Shim, and H. S. Song, Spin-2 particle polarization, *J. Korean Phys. Soc.* **25**, 576 (1992).

[26] V. Devanathan, *Angular Momentum Techniques in Quantum Mechanics*, Fundamental Theories of Physics (Springer Netherlands, 2005).

[27] S. U. Chung, *SPIN FORMALISMS*, Tech. Rep. CERN-71-08 (CERN, 1971).